A reprint from

OPTICAL ENGINEERING

ISSN 0091-3286

Off-axis laser detection model in coastal areas

Nathalie Roy
Françoise Reid

Optical Engineering 47(8), 086002 (August 2008)

P.O. Box 10, Bellingham, Washington 98227 USA. Telephone 360/676-3290

Off-axis laser detection model in coastal areas

Nathalie Roy
Françoise Reid
Defense Research and Development
Canada Valcartier
2459 Pie XI Boulevard North
Québec, Canada, G3J 1X5
E-mail: nathalie.roy@drdc-rddc.gc.ca

Abstract. Relatively inexpensive laser-guided weapons were identified as an important threat to naval platforms operating in littoral environments. Countermeasures (CM) developed against laser-assisted threats in air and land environments are all based on accurate threat detection. Due to the limited performance of current laser detecting capabilities applied to large maritime platforms, there are no known CMs that can be used to protect them. We present a new far off-axis laser detection approach for minimizing the number of laser sensors required to protect a ship. A model predicting the detection of aerosol scattering in the spectral band used by laser threats, exploiting the high humidity conditions present in maritime environments, is described, as well as its limitations and some preliminary results regarding its validation. © *2008 Society of Photo-Optical Instrumentation Engineers.* [DOI: 10.1117/1.2969119]

Subject terms: off-axis laser detection; scattering; coastal areas; aerosol; prediction model.

Paper 080263R received Apr. 5, 2008; revised manuscript received Jun. 4, 2008; accepted for publication Jun. 21, 2008; published online Aug. 20, 2008.

1 Introduction

When ships operate in coastal areas, there are no coastal surveillance systems onboard to inform the Commander of the presence of hostile forces hidden on the coast. Some of them can use relatively inexpensive laser-guided weapons against the ship, mainly laser beam riders and laser-designated missiles.

Protection systems developed against laser-assisted threats in air and land environments are all designed to detect laser radiation between 3 to 6 m off-axis. If placed at the center of a 14-m aircraft or land vehicle, they would be able to detect any laser beam that hits the platform, since most energy detected by the laser warning receiver (LWR) comes from the main beam, which is mainly included in the first 6-m off-axis. Such LWRs are perfectly adapted to land and air platforms but not for warship applications, where 70 to 100-m off-axis distances are required.[1,2]

Lasers used for weapons guidance can aim at very specific areas of the ship, which can be located several meters or tens of meters away from the LWR location. LWRs specifically designed for this application will work outside the main beam, where detection is due either to off-axis aerosol scattering or port scattering (due to output optics). Laser radiation is scattered from aerosols (dust particles and water droplets) along the entire beam path, creating a spatially distributed radiation source, which creates an angular distribution of the irradiance at the LWR. The contribution of aerosol or port scattering depends on the laser type and wavelength, as well as the atmosphere characteristics through which the beam propagates. Figure 1[1] shows the sum and the relative contributions of direct, aerosol, and port scattered radiation as a function of miss distance from the beam of a typical 1.06-μm laser designator in an urban area.

Based on Fig. 1, one could think that reaching the suitable off-axis detection would simply be achieved by further reducing the LWR detection threshold. Unfortunately, this is very difficult to do because the detection threshold of the existing LWR is already near the limit achievable to maintain an acceptable false alarm rate. The detection threshold is mostly limited by the strong natural background radiation that is present in daylight conditions, the field of view (FOV) of the detectors, the width of waveband covered, and the number of false alarms tolerable.

The optimization of the detection parameters, coupled to the fact that in the maritime environment the aerosol scattering level has a tendency to be higher (due to the presence of more droplets in the atmosphere), should permit us to substantially extend the LWR off-axis capability. To determine the optimum design for the laser warning receiver and to predict its performances in coastal areas, an off-axis aerosol scattering model was developed. Some simplifica-

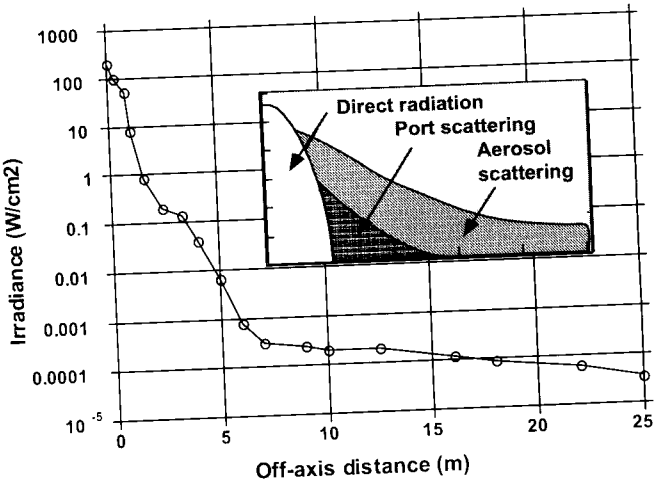

Fig. 1 Typical laser off-axis signature at 3 km (λ=1.06 μm, 30 mJ/laser pulse, divergence=0.6 mrad).

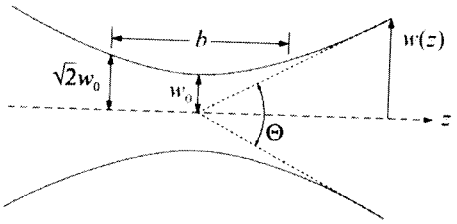

Fig. 2 Gaussian beam spot size.

tions have been made such that its application in the spectral band used by laser threats is relatively simple. This model takes into account the features of the lasers used for weapons guidance, the background aerosol quantity and size distribution according to the meteorological conditions, some geometrical considerations, and finally, some characteristics of the detection system used.

In a real detection scheme, aerosol scattering is combined with direct radiation, and port scattered and background radiation. The relative contribution of these sources is a function of the miss distance from the laser threat, the daytime, and the meteorological conditions. Our model only includes contributions from direct radiation and aerosol scattering, as described in Secs. 2–5.

In this work, these four sources of radiation (direct, aerosol scattering, port scattering, and background radiation) are briefly described, and our off-axis detection model is presented as well as its limitations, and some preliminary results regarding its validation.

2 Direct Radiation

To model the direct radiation, we assume that the laser beam is Gaussian. According to this assumption, the laser beam power P_{direct} (in watts) at a distance z_{tot} from the beam waist that is collected by a LWR collecting optics of diameter D, for an off-axis distance d, is given by:

$$P_{\text{direct}}(D,d,z_{\text{tot}}) = \frac{P_0 D^2}{\left[\left(d+\frac{D}{2}\right)^2-\left(d-\frac{D}{2}\right)^2\right]} \times\left[\exp\left[\frac{-2(d-D/2)^2}{w(z_{\text{tot}})^2}\right]-\exp\left[\frac{-2(d+D/2)^2}{w(z_{\text{tot}})^2}\right]\right][\exp(-\alpha_{\text{ext}}z_{\text{tot}})] \times[\exp(-\alpha_{\text{mol}}z_{\text{tot}})]t_{\text{syst detection}}, \quad (1)$$

where P_0 is the total power emitted by the beam and $w(z_{\text{tot}})$ is the radius of the spot size of the beam at a distance z_{tot} corresponding to the laser to the LWR distance along the laser beam axis. The last three factors in Eq. (1) represent respectively the absorption by the background aerosols $[\exp(-\alpha_{\text{ext}}z_{\text{tot}})]$ and the molecules in the atmosphere $[\exp(-\alpha_{\text{mol}}z_{\text{tot}})]$, and the losses into the optical components of the detection system and the filter transmission ($t_{\text{syst détection}}$). As illustrated in Fig. 2, for a Gaussian beam propagating in free space, the spot size $w(z)$ has its minimum value w_0 at one location along the beam axis, known as the beam waist. For a beam of wavelength λ at a distance z along the beam from the beam waist, the variation of the spot size is given by:

$$w(z) = w_0\left[1+\left(\frac{z}{z_0}\right)^2\right]^{1/2}, \quad (2)$$

where the origin of the z axis is defined, without loss of generality, to coincide with the beam waist. The Rayleigh range can be defined in function of this parameter:

$$z_0 = \frac{\pi w_0^2}{\lambda}. \quad (3)$$

The spot size $w(z)$ approaches a straight line for $z \gg z_0$. The angle between this straight line and the central axis of the beam is called the divergence of the beam. It is given by:

$$\theta_{\text{beam}} \approx \frac{\lambda}{\pi w_0}. \quad (4)$$

So, knowing the laser beam divergence and the laser wavelength, it becomes possible to retrieve w_0, z_0, the spot size, and thus the contribution of the direct radiation.

3 Port Scattering

The intensity of the port scattering depends on the construction method of the laser, as well as its wavelength, operating modes, optical quality, and port cleanliness. There is currently no known physical model that can be used to predict adequately the intensity of the port scattering. However, we know from our measurements that its scattered intensity decreases very rapidly with the off-axis distance, and that the port scattering is only visible when the laser optics output is within the FOV of the LWR or very close to it. Therefore, we did not include the port scattering contribution in our model, as we believe that the impact on the precision of our model is negligible as long as we keep the laser port outside the field of view of the detecting system. We limited our prediction model calculations to the scattering points that respect that criterion.

4 Model for Laser Beam Scattering on Maritime Aerosols

The amount of radiation received by an observer looking through the Earth's atmosphere depends on the wavelength of the radiation and the number, size, shape, composition, and distribution of the atmospheric constituents.[3,4] Each atmospheric constituent scatters or absorbs the incident radiation according to its own properties, and the incident radiation may have been previously scattered by another constituent. To model in a simple relation the laser beam scattering on background aerosols, it is necessary to make some simplifying assumptions.

1. Each scattering event is independent, and therefore the scattering properties of a given type of particle distribution can be represented by an integral over the size distribution.
2. The particle distribution is homogenous over the volume concerned.

3. The multiple scattering contribution is negligible in regards with the first scattering order contribution.
4. The particles can be approximated as spherical, so Mie theory can be applied.
5. The angular scattering distribution $p(\beta)$ (the phase function) will give the directional distribution of the radiation scattered by the aerosol under consideration: it is normalized over 4π sr so that:

$$\int_0^{2\pi}\int_0^{\pi} p(\beta)\sin\beta d\beta d\phi = 1, \tag{5}$$

where $p(\beta)$ is calculated using the Mie theory; it is a function of the wavelength, the particle diameter, and its complex refractive index.
6. The LWR sensor looks toward the laser beam axis.

According to these assumptions, for good visibility conditions, the power collected by a sensor (P) in watts coming from the laser beam scattering on the background aerosols can be predicted using a simple relation that depends on the laser features, the receiver features, some geometrical considerations, the air molecule content, and the background aerosol's quantity and size distribution:

$$\begin{aligned} P = &[P_0(c\tau)a\alpha_{\text{ext}}p(\beta_i \pm \sigma_d/2)] \\ &\times\{\exp[-\alpha_{\text{mol}}(z+R)]\exp[-\alpha_{\text{ext}}(z+R)]\} \\ &\times\left[t_{\text{syst detection}}\left(\frac{AFr_{\text{noobtured}}}{d^2/\sin^2\beta_i}\right)F_{\text{laserpulse}}F_{\text{laserbeam}}\right]. \end{aligned} \tag{6}$$

Parameters of Eq. (6) are defined in Table 1. The terms in the first bracket in Eq. (6) correspond to the fraction of the laser beam scattered by the background aerosols in the direction of the sensor; while the second and third brackets represent respectively the laser beam attenuation by the atmospheric constituents and the fraction of energy collected by the detection system, according to the geometrical features and receiver parameters.

In the following sections, we study more carefully how the background aerosol's quantity and size distribution, the air molecule content, the geometrical considerations, the laser used for weapons guidance features, and the detection system characteristics affect the amount of scattered light collected by a LWR.

4.1 *Amount of Scattered and Absorbed Light: Impact of Aerosols and Air Molecules*

The lost of intensity ΔI of a laser beam propagating along z can be written as:

$$\Delta I = -\alpha_{\text{ext}} I \Delta z, \tag{7}$$

where α_{ext} is the extinction coefficient. It represents the lost of light per unit length and it is expressed in Eq. (6) by the factor $\exp[-\alpha_{\text{ext}}(z+R)]$. The losses have two origins: the light is either scattered or absorbed by the molecules $[(\alpha_{\text{ext}})_{\text{molecule}}]$ and by the aerosols $[(\alpha_{\text{ext}})_{\text{aerosol}}]$. As described in the following sections, only the light scattered and absorbed by the aerosols will be taken into account in our model, the molecular scattering and absorption being negligible at the wavelength of 1.06 μm used. Therefore, to shorten the notation in this work, we have chosen to define α_{ext} as the extinction coefficient due to the aerosols.

Table 1 Definition of Eq. (6) parameters.

Parameters	Definition	Units
α_{ext}	Aerosols extinction coefficient	m^{-1}
α_{mol}	Molecular selective absorption coefficient	m^{-1}
β	Scattering angle	rad
σ_d	Field of view of the sensor (full angle)	rad
τ	Laser (used for weapons guidance) pulse width	s
a	Albedo (fraction of the aerosol extinction coefficient that is scattered while the other part is absorbed)	—
A	Total surface of the collecting optics	m^2
c	Light speed	3×10^8 m/s
d	Off-axis distance	m
$F_{laserbeam}$	Fraction of the laser beam collected by the detection system optics given by Eqs. (13) and (14) in Sec. 4.2.1	—
$F_{laserpulse}$	Fraction of the laser pulse collected by the detection system optics given by Eqs. (15) and (16) in Sec. 4.2.2	—
$Fr_{noobtured}$	Fraction of the collecting optics total surface that it is not obstructed	—
p	Aerosol phase function in sr^{-1} (fraction of the laser beam that is scattered in a direction β). This function should be normalized such that: $\int_0^{2\pi}\int_0^{\pi}p(\beta)\sin\beta d\beta d\phi=1$.	sr^{-1}
P_o	Output power for each laser pulse	W
R	Distance between the scattered point and the detection system	m
$t_{syst\ detection}$	Transmission of the detection system (lens+filters)	—
z	Distance between the laser optics output and the scattered point	—

4.1.1 *Aerosol extinction and meteorological conditions*

The suspended particles are collectively known as aerosols, and their contribution is called aerosol scattering. Because of their diversity, aerosol particles have a wide range of sizes. However, the most important ones for optical scattering are so because their size is comparable to the wavelength being scattered, for typical aerosol size distributions.

Therefore, for calculating aerosol extinction, the Mie theory is used. This theory of scattering is a general solution that covers the scattering of electromagnetic radiation by a homogeneous sphere for all wavelengths of radiation and spheres of all sizes and refractive indexes.

Another important parameter regarding aerosol extinction is the single scattering albedo a, defined by the ratio α_s/α_{ext}, where α_s is the scattering coefficient. It corresponds to the fraction of the aerosol extinction coefficient that comes from scattering, while the other part is absorbed.

The amount of scattered light by background aerosols is proportional to the scattering coefficient α_s, which is equal to $a\alpha_{ext}$. In our model, the extinction coefficient is calculated from the visibility "vis" measurement. The visual range (visibility) is defined as the distance at which the test object is just distinguishable from the background. Based on observations, the visibility is defined for a transmission of 2% at a wavelength of 0.55 μm[5] by:

$$\text{vis} = -\frac{1}{(\alpha_{ext})_{\text{at } 0.55\ \mu\text{m}}} \ln(0.02) = \frac{3.912}{(\alpha_{ext})_{\text{at } 0.55\ \mu\text{m}}}. \quad (8)$$

Knowing the visibility, α_{ext} at 1.06 μm is extrapolated from α_{ext} at 0.55 μm.

The phase function, the fraction of the laser beam that is scattered in direction β, and the albedo a are calculated in our model using the Mie theory in conjunction with the particle size density distribution proper to the meteorological conditions. While other scattering on background aerosols models[6,7] are based on the Shettle and Fenn[8] background aerosol size distribution model, which depends only on four parameters: visibility, ambient temperature, relative humidity, and aerosols types (rural, urban, or maritime), the scattering on background aerosols model we used is more accurate and requires 12 input parameters related to the meteorological conditions, for the calculation of the sea-surface generated particle size distribution, according to one of the four available predefined distributions sets. They are Kel (North Atlantic) and NAM for the maritime conditions; IRELAND and MEDEX for respectively the coastal areas near the Ireland coast and the North-American coast. The 12 parameters as well as their units and their range of values are listed in Table 2.

Figure 3 compares the background aerosol size distribution (dN/dr) at 10 m above sea surface obtained with the Shettle and Fenn model with the one obtained with our model using MEDEX predefined distribution for a representative scenario mP-mT, which is a mix of a maritime-polar with a maritime-tropical air mass (for more details, see the note at the bottom of Table 2). In the Shettle and Fenn model,[8] the aerosol size distribution is calculated as the sum of two lognormal functions. The relative number of particles in each mode, the mode mean radius, and the geometric standard deviation functions depend only of the aerosol type (maritime, urban, or rural) and the relative humidity. In the MEDEX distribution model,[9] the coastal aerosol size distribution is calculated as the sum of four modified lognormal functions with coefficients of the various modes parameterized as functions of the relative humidity, the wind speed, and the fetch (the length of water over which the wind has blown). The fourth mode has been introduced to model the largest sea spray particles. The details of these two aerosol size distribution models are described in Appendix A in Sec. 9.

Table 2 Meteorological conditions used for the background aerosol quantity and size distribution calculations.

Parameters	Units	Min	Max
Atmospheric pressure	mb	800	1200
Air temperature	°C	−20	40
Sea temperature	°C	−5	40
Relative humidity	%	20	98
Wind speed	m/s	0.1	20
Average wind speed (24 hrs)	m/s	0	20
Fetch (only used in coastal model)[a]	km	3	120
Visibility	km	0	200
Air mass parameter[b] (AMP)	—	1	20
Wave height	m	0	10
Type of environment (ocean=0, coastal area=1)	—	0	1
Height of temperature/humidity/ pressure measurement	m	3	40
Height of wind speed measurement	m	3	40

[a]The fetch corresponds to the length of water over which the wind has blown.

[b]An air mass is a large volume of air having fairly uniform characteristics of temperature, atmosperic pressure, and water vapor content. Air masses are classified according to their temperature and moisture content. The temperature characteristics of an air mass are defined by the terms arctic (A), polar (P), tropical (T), and equatorial (E). The moisture content of an air mass is defined by the terms maritime (m) and continental (c). Maritime air is a moist air mass, whereas continental air is relatively dry. If this parameter is unknown, we must set its value to −99. The program will in this case use only the visibility measurement to make its calculations.

Figure 3 clearly demonstrates that the particle size distribution is affected by the choice of model used for its calculation. The particle radius peak is larger in the Shettle and Fenn maritime model with a value of 0.17 μm, followed by the particle size obtained with the MEDEX model with a radius peak at 0.03 μm, while the Shettle and Fenn urban and rural models give pretty much the same size distribution with a radius peak located around 0.015 μm. The predicted power collected by a sensor coming from the aerosol scattering [Eq. (6)] will be affected by an error on the particle size distribution retrieved since, as already mentioned, Mie calculations for the extinction coefficient (α_{ext}) and the phase function (p) directly depend on the particle size profile.

Figure 4 shows a graph of phase functions in the function of the scattering angle for the four particle size distributions illustrated in Fig. 3. We can observe large discrepancies of the phase function values retrieved for scattering

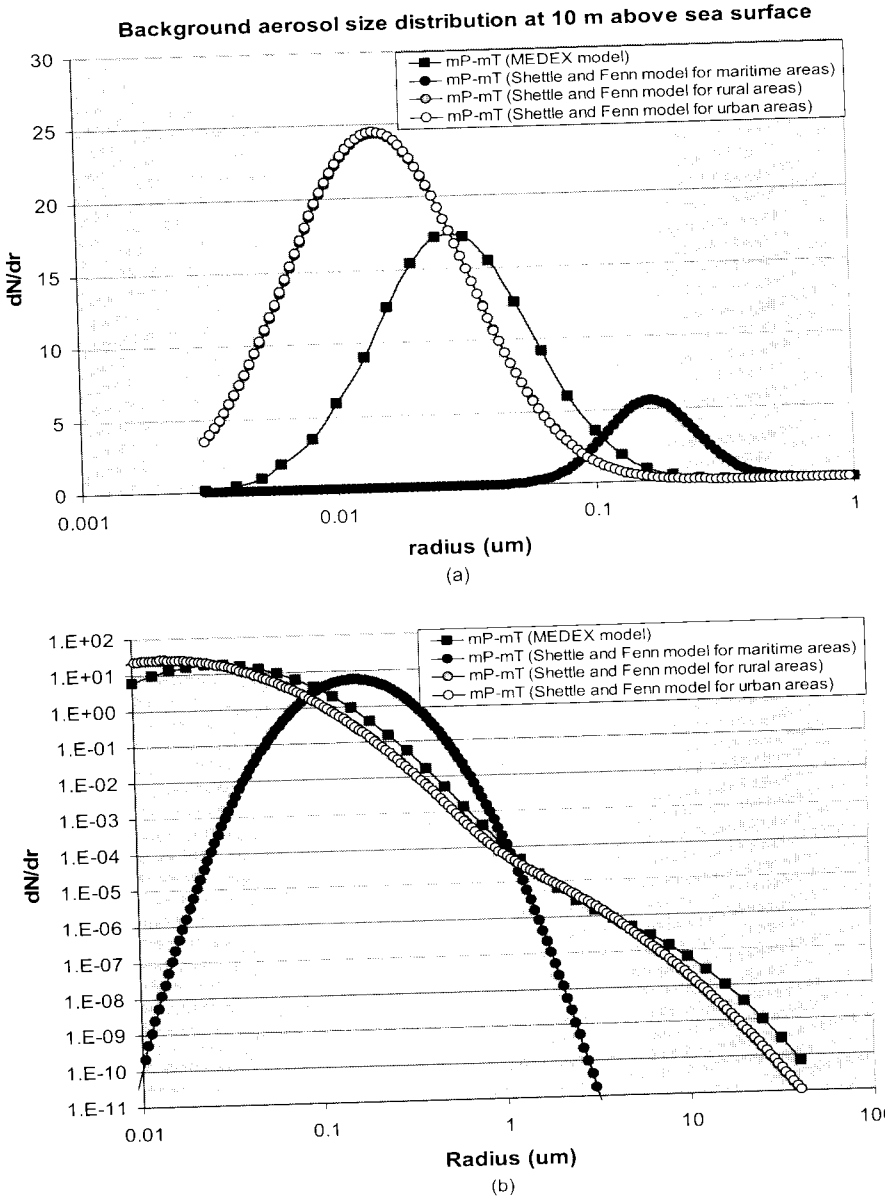

Fig. 3 Comparison of background aerosol size distribution at 10 m above sea surface obtained with the Shettle and Fenn model and the MEDEX model for a representative scenario mP-mT in the North American basin in autumn: (a) on a linear scale and (b) on a logarithmic scale.

angles smaller than 10 deg. For the smaller scattering angles, the larger values of the phase function observed for the MEDEX model can be explained by the fourth mode introduced to model the largest sea spray particles. The presence of those larger particles can be clearly seen in Fig. 3(b). For larger scattering angles, the difference between the four curves is not so important. If, for example, we set the maximum off-axis detection distance to 70 m, scattering angles larger than 10 deg will correspond to detection distance smaller than 400 m; while for a smaller off-axis detection distance, they will correspond to detection distances even smaller. Consequently, it is essential to model well the background aerosol size distribution to predict efficiently the power collected by a sensor coming from the laser beam scattering on the background aerosols over all the distances covered between the ship and the coast.

4.1.2 *Molecular Rayleigh scattering*

Since molecules are small compared to the wavelength of the incident radiation, molecular scattering can be calculated using the Rayleigh scattering theory from:[10]

$$\alpha_{\text{Rayleigh}} = 1.33 \times 10^{-5}\left(\frac{\lambda}{0.532}\right)^{-4}. \tag{9}$$

In the near-infrared and IR spectrum, the aerosol extinction coefficient largely predominates over the Rayleigh extinction coefficient, even for good visibility conditions. For example, at $\lambda = 1.06\ \mu$m, we obtain $\alpha_{\text{Rayleigh}} = 8.44 \times 10^{-7}\ \text{m}^{-1}$; while for a visibility of 30 km,

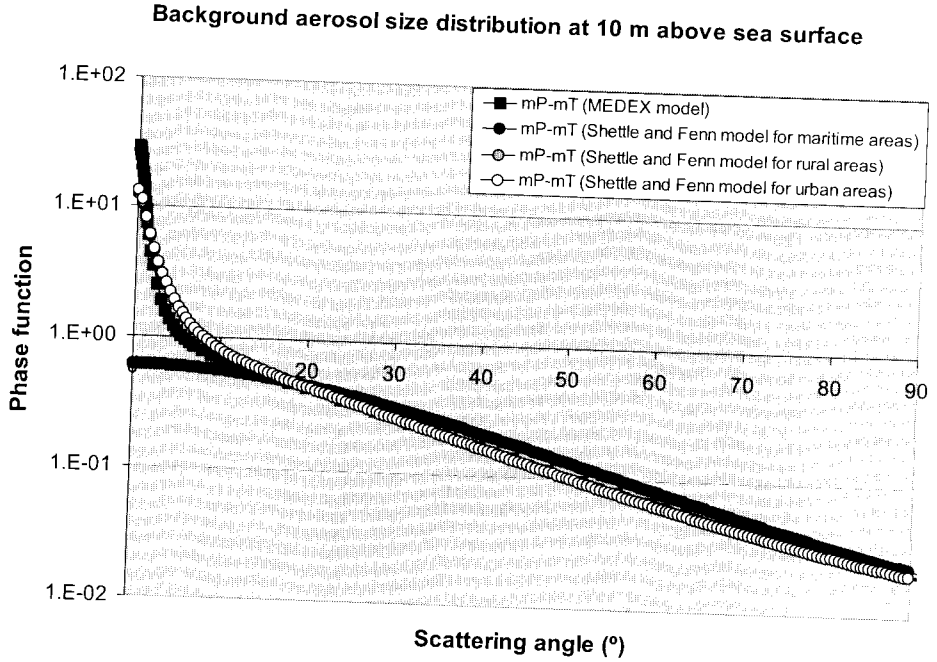

Fig. 4 Comparison of phase function for a background aerosol size distribution at 10 m above sea surface obtained with the Shettle and Fenn model and the MEDEX model for a representative scenario mP-mT in the North American basin in autumn.

$\alpha_{ext} = 1.30 \times 10^{-4}$ m^{-1}. So, we can neglect the contribution of the molecular Rayleigh scattering without affecting the precision of our prediction model.

4.1.3 *Molecular selective absorption coefficient*

The laser beam is also absorbed by air molecules in narrow spectral bands with a molecular selective absorption coefficient α_{mol}. For a ground-based application, selective molecular absorption is negligible in the spectrum area mostly used in laser-designated weapons, which is around 1.06 μm.

Absorption by molecules is sometimes called "true absorption," to emphasize its difference from extinction due to scattering; or "selective absorption," to emphasize its concentration in narrow spectral bands. The main absorbers in the visible spectrum are ozone (which absorbs in the Chappuis bands, in the orange part of the spectrum), water vapor (several bands in the longer-wavelength regions, noticed mainly under very humid conditions, hence the name "rain bands"), and oxygen (which produces Fraunhofer's A and B bands).

Equation (6) includes a molecular selective absorption factor α_{mol} that is negligible at a wavelength of 1.06 μm, but for others wavelengths this is not necessarily the case. For example, a CO_2 and water vapor continuum can significantly affect the propagation at 10.6 μm. The absorption coefficient is defined as a function of the air temperature T, the relative humidity Rh, and the atmospheric pressure. The molecular extinction coefficient depends on the absolute water content ρ expressed in g/m^3. The relation between T (°K), $Rh(\%)$, and ρ (g/m^3) can be written as:

$$\rho(T,RH) = \frac{217}{T}\frac{Rh\%}{100}6.11\exp\left[\frac{7.5(T-273.15)}{237.3+(T-273.15)}\right]. \quad (10)$$

For low water vapor contents, the extinction is mainly caused by the presence of CO_2 molecules, and the extinction can be modeled, for example, at 10.6 μm with the following equation:

$$\alpha_{mol}(10.6\ \mu\text{m}) = 0.0003409\rho^2 + 0.004222\rho + 0.08568. \quad (11)$$

4.2 *Impact of Some Geometrical Considerations*

When we predict the amount of energy coming from the scattering on background aerosols, we should take into account the geometrical considerations related to the field of view of the sensor, the off-axis distance of the laser used for weapons guidance, and the range of scattering angles detected by the LWR. A pulse width with a small divergence fills a volume quasicylindrical in the space. In reality, it is more like a truncated pyramid. Depending of the parameters previously stated, the surface occupied by the laser beam as well as the laser pulse will be totally or partly contained inside the field of view sustained by the sensor. To take into account the fraction of the laser beam and the fraction of the laser pulse collected by the detection system, we have to multiply Eq. (6) by two correcting factors: $F_{laserbeam}$ and $F_{laserpulse}$.

4.2.1 *Correction for the fraction of the laser beam collected by the detection system optics: $F_{laserbeam}$*

When the laser divergence is given by θ_{beam}, far from the laser source, as illustrated in Fig. 5, the diameter of the laser beam D_{beam} can be expressed as:

$$D_{beam} = z\theta_{beam}. \quad (12)$$

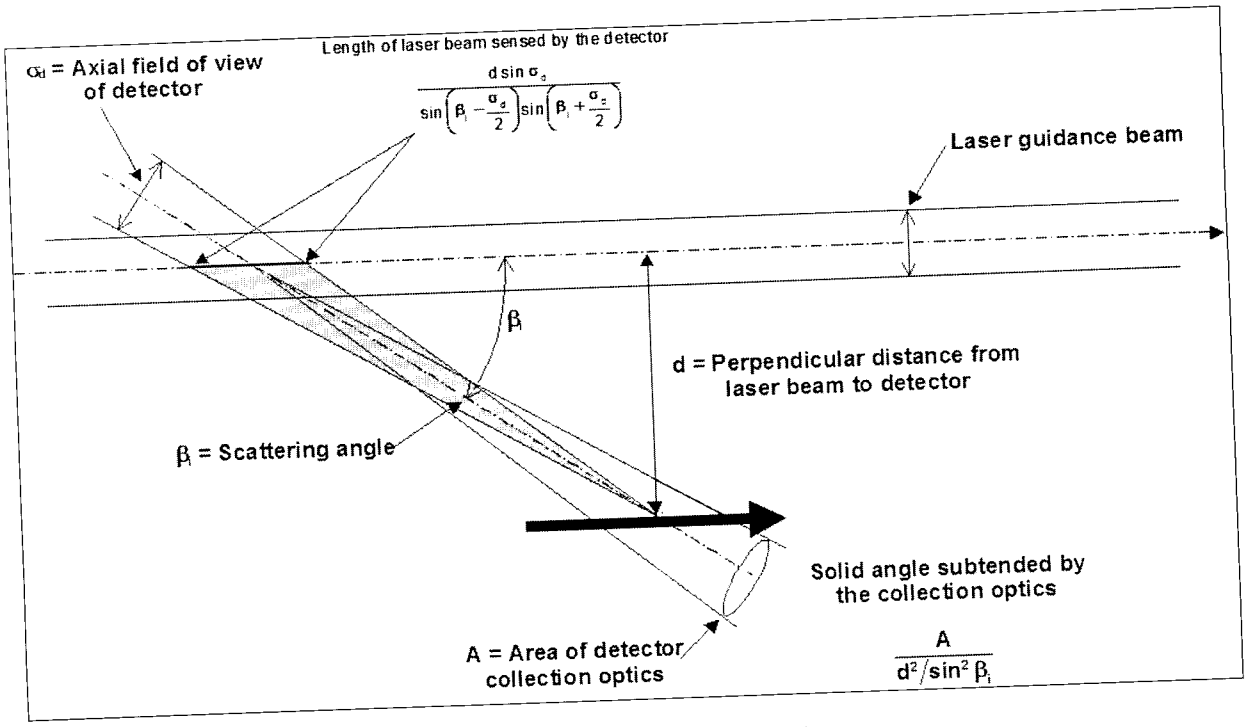

Fig. 5 Fraction of the area collected.

The collecting optics can collect totally or partly the area occupied by the beam at a distance R. The fraction of the area collected can be expressed in function of the parameters already defined in Table 1:

$$F_{\text{laserbeam}} \approx \frac{z\theta_{\text{beam}} R\sigma_d Fr_{\text{noobtured}}}{\pi(z\theta_{\text{beam}})^2/4} \approx \frac{R\sigma_d Fr_{\text{noobtured}}}{z\theta_{\text{beam}}}. \quad (13)$$

Moreover,

$$\text{if} \quad \frac{R\sigma_d}{z\theta_{\text{beam}}} \geq 1, \quad \text{we should set } F_{\text{laserbeam}} \text{ equal to } Fr_{\text{noobtured}}. \quad (14)$$

4.2.2 *Correction for the fraction of the laser pulse collected by the detection system optics: $F_{\text{laserpulse}}$*

To calculate the fraction of the laser pulse collected by the detection system optics, we should apply the sinus rule on the gray triangle of Fig. 6. It is then possible to find an expression for the length of the laser beam sensed by the detector ($L_{b\ \text{sensed}}$) in function of the parameters already defined in Table 1:

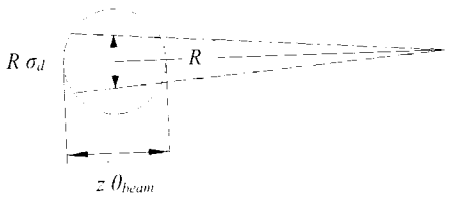

Fig. 6 Fraction of the laser pulse collected by the detection system optics.

$$L_{b\ \text{sensed}} = \frac{dFr_{\text{noobtured}} \sin \sigma_d}{\sin(\beta - \sigma_d/2)\sin(\beta + \sigma_d/2)}. \quad (15)$$

Depending on the off-axis distance, the field of view of the sensor, and the range of scattering angle detected, the sensor will collect the laser pulse totally or partially. The fraction of the laser pulse seen by the sensor is given by:

$$F_{\text{laserpulse}} = L_{b\ \text{sensed}}/(\tau c), \quad (16)$$

where c corresponds to the light speed in m/s and τ to the laser pulse width in s.

For certain cases, the detection system collects the scattering on background aerosols over a length longer than the one associated with a single laser pulse. For those cases, the signal measured on the sensors corresponds to the summation of the signal coming from different laser pulses.

The last assumption we have made in our model is that the photon flight time between their emission at the laser output optics and their detection is the same for every scattering point included in the field of view of the sensor.

4.3 *Laser Features and Characteristics of the Detection System*

The third bracket of Eq. (6) is present to take into account some geometrical considerations described in Sec. 4.2, but also to account for the characteristics of the laser and detection system.

The amount of scattered light depends on the features of the laser used for weapons guidance. More specifically, it depends on its pulse output power (P_o), its divergence, and

its pulse width (τ). Its wavelength affects the calculation of the aerosols extinction coefficient (α_{ext}), the molecular selective absorption coefficient (α_{mol}), the phase function (p), and the albedo (a).

Our model directly depends also on some characteristics of the detection system: the total surface of the collecting optics (A), the fraction of this surface that is not obstructed ($Fr_{noobtured}$), the field of view of the sensor (σ_d), and the lens and filter transmissions of the detection system grouped in Eq. (6) in a single term: $t_{syst\ detection}$.

5 Background Radiation

Background radiation comes from sky radiance. Its contribution depends on solar irradiance on the Earth's surface, which possesses a strong spectral dependency.[11] Moreover, because of its aerosol and molecular content, the air mass between the sensor and the surface will absorb or scatter some radiation. Radiation from the surface and external sources like the sun can also be scattered, or even multiply scattered, toward the sensor, augmenting the apparent radiance. It is thus crucial to properly consider the radiative coupling between extraterrestrial sources, the air, and the sea surface.[12,13]

Background radiation depends on many factors such as the solar angle, nebulosity, relative humidity, the sun azimuth relative to the observation direction, daytime, and aerosol concentration into the atmosphere. Some theoretical background radiation models exist to predict its level. The most used is probably MODTRAN, a computer program designed to model atmospheric propagation of electromagnetic radiation from 100 to 50,000 cm^{-1} with a spectral resolution of 1 cm^{-1}. However, MODTRAN used alone does not provide a sufficient result, as the propagation between the sea surface and the detector has also to be taken into account in our model to predict the amount of radiation arriving at a sensor. For that, it would be necessary to add a functionality to MODTRAN: a sea bidirectional reflectance distribution function (BRDF).[12] Moreover, since MODTRAN calculates the spectral irradiance for a single sight line assuming a uniform nebulosity, it would be necessary to sum many sight lines to take into account all the angles covered by the field of view of the sensor and to average results to simulate a nonuniform nebulosity or a mid-cloud sky.

Real-time experimental measurements are surely the most representative values for background radiation, since they take into account all parameters that can influence its level for a sight line, including environmental features, meteorological conditions, and LWR characteristics. Moreover, in real laser-assisted threat detection schemes, the background level can usually be easily subtracted. This is why at this first stage we have not theoretically modeled the background radiation.

For example, in the DRDC-Valcartier CM system against laser threats, the detection threshold is currently established according to the natural background radiation level measured by the LWR. To verify if a signal level higher than the threshold corresponds or not to a false alarm, the periodicity of the signal is analyzed. In the near future, further improvements of the sensors could allow us to perform a direct background radiation subtraction between two detected laser pulses.

6 Limitations of the Model

The model presented is based on some simplifications that can affect the prediction precision. In this section, we describe the limitations of the model and we explain their impacts on the results obtained.

6.1 *Prediction for Small Scattering Angles*

Our model does not provide results for small scattering angles, where we can expect to measure the port scattering contributions. However, it should be noticed that for those angles, it should be easy to detect the laser threat presence, since port scattering should be more important by 2 orders of magnitude than aerosol scattering. Consequently, limitation regarding the small scattering angle should not significantly affect the laser warning receiver model prediction performances. For example, for an off-axis distance of 4 m, our model begins its calculations for a scattering angle β of 2 deg (see Fig. 6); while for an off-axis distance of 76 m, it begins its calculations for a scattering angle of 4 deg when the field of view of the LWR is fixed to 3.75 deg and the laser to ship distance to 2.5 km.

6.2 *Altitude of the Prediction*

Currently in our model, it is only possible to calculate the aerosol extinction and the phase function from the sea surface up to 10 m above water for a single altitude. Calculations for altitudes higher than 10 m will require us, in a second phase, to apply the theory of turbulent transport of particles to estimate the vertical variation of extinction. Since the aerosol extinction and the phase function vary with altitude, if the altitude of the laser beam is not constant over the ocean surface, we can expect small discrepancies between the prediction model results and the real values that should be measured. When the laser beam is closer to the sea level, we can expect to detect a higher level of signal than the one predicted, since the relative humidity and the number of sea spray particles increase. For a higher scattering point than the one used in the prediction model, we should observe the opposite behavior.

6.3 *Multiple Scattering Contribution*

Multiple scattering contributions can usually be neglected compared to single scattering in good visibility conditions. However, in cases of fog or precipitations, this assumption no longer stands, and the off-axis aerosol scattering may be higher or lower than the one predicted by our model based on single scattering approximation, depending on if the increase of the signal is superior to its decrease related to the extinction attenuation factor $\exp[-\alpha_{ext}(z+R)]$ in Eq. (6). The multiple scattering contributions will increase with the background aerosol concentration, the field of view of the sensor, and with the distance between the first scattering and the LWR.

6.4 *Separation between Discrete Scattering Points*

Our prediction model considers the background aerosol volume included inside the field of view of the detection

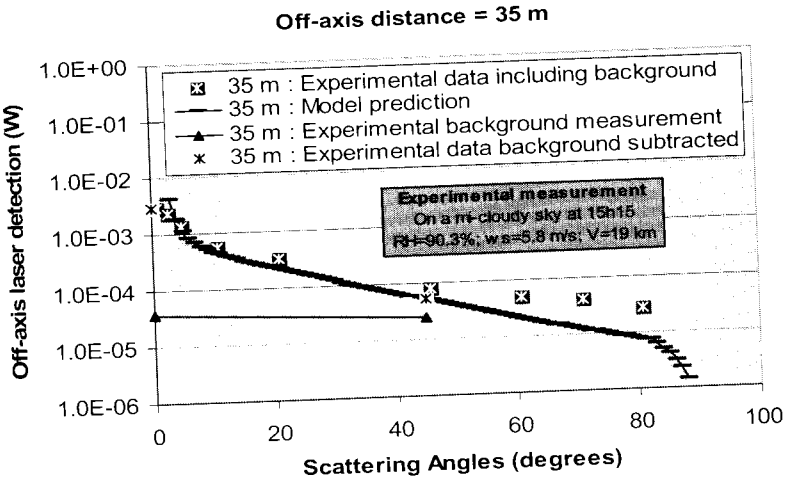

Fig. 7 Comparison of our model prediction with the experimental data in function of the scattering angles for an off-axis distance of 45 m and a laser-to-ship distance of 2.5 km. The relative humidity RH was 89.9%, the wind speed (ws) was 5 m/s, and the visibility (V) was 19 km.

system as a series of points equally angularly spaced that scatters the laser beam toward the LWR inside scattering angles included between $(\beta-\sigma_d/2)$ and $(\beta+\sigma_d/2)$, where σ_d corresponds to the field of view of the sensor and $\beta = \arctan(d/(z_{\text{tot}}-z))$, d corresponds to the off-axis distance, z_{tot} to the distance between the laser output and the LWR along the laser beam axis, and z to the distance between the laser output and the scattering point studied.

The product of the phase function and the solid angle has been obtained by considering each scattering point separately and by summing the contribution of each of them:

$$\frac{\sum_{\beta_i=\beta-\sigma_d/2}^{\beta_i=\beta+\sigma_d/2} p(\beta_i)\frac{AFr_{\text{noobtured}}}{d^2/\sin^2\beta_i}\Delta\beta_i}{\sigma_d}. \tag{17}$$

Ideally, the scatter model should break the beam contained in the sensor's FOV into a number of discrete scatter points equally spaced along the beam axis. Then, it should calculate the scattered energy associated with each one that is scattered into the detector, apply the appropriate time shift, and sum them incoherently after having taken into account the LWR characteristics.

In our model, since the beam contained in the sensor's FOV is broken into a number of discrete scatter points spaced equally angularly instead of spaced equidistant along the beam axis, more scattering points for shorter distances from the LWR in our model are considered in the calculation of the total power collected by the LWR than scattering points from farther distances from the LWR. So, the part of the sensed beam closer to the LWR will influence more the predicted power obtained from our model than the sensed beam farther to the LWR. This will eventually lead to some errors.

The discrepancies between both models, the one with discrete scatter points equally spaced along the beam axis and the one with discrete scatter points equally angularly spaced, will be more important for smaller scattering angles, since it is for those angles that the phase function and the solid angle vary most rapidly.

6.5 *Signal-to-Noise Ratio Calculations*

Modeling natural background levels is not absolutely essential, since in real laser-assisted threat detection schemes, the background level can be easily subtracted. However, performing purely theoretical calculations of the laser warning receiver performances based on signal-to-noise ratio is only possible if the natural background level is modeled or its level is fixed according to experimental measurements or to literature reference values. Such calculations would allow us to determine the optimum field of view of laser warning receivers, taking into account the number of sensors that should be on the ship and the minimization of the relative influence of the background fluctuations regarding the off-axis aerosol scatter signal level to decrease the false alarm rate.

7 Validation

A measurement campaign was made by DRDC-Valcartier near the harbor of Halifax in October 2006. The specific objective of this trial was to measure how far off-axis we can record a laser signal in a maritime environment using current capabilities for different atmospheric conditions and off-axis distances. Figure 7 illustrates one example of the results obtained for an off-axis distance of 35 m and a laser-to-ship distance of 2.5 km. The white stars in black squares correspond to the experimental data obtained when the laser was in operation and the signal on the detector was peaked. By peaked, we mean that the sensor operator looked for the position on a vertical axis for which the signal recorded was maximum. Each white star in black squares represents the laser signal recorded from a portion of the laser beam located more or less far away from the laser output, which can be related to a specific angle of

Table 3 Characteristic of the aerosol model for lower atmosphere. The r_i mode radii correspond to moderate humidities (70 to 80%); Values of r_i as function of humidity are given in Table 4.

	Size distribution			
Aerosol model	N_i	r_i^*	s_i	Type
Rural	0.999875	0.03	0.35	Mixture of water-soluble and dust-like aerosol
	0.000125	0.5	0.4	
Urban	0.999875	0.03	0.35	Rural aerosol mixture with soot-like aerosol
	0.000125	0.5	0.4	
Maritime	1	0.3	0.4	Sea salt solution in water

detection in a simple relation: $\beta=\arctan[d/(z_{tot}-z)]$. The black triangles correspond to the background level measurements. They have been obtained for the same geometry as the white stars in black squares, but when the laser was not in operation. The agreement between our prediction model and our experimental data after the background level subtraction (black stars in white squares) is very good, even for scattering angles larger than 30 deg for which the background level has about the same magnitude as the off-axis detection, coming mainly from the laser beam scattering on the aerosols.

The discrepancies between the model prediction and the experimental data can be explain as follows.

1. The fluctuations of the meteorological conditions between the meteo station and the scattering point, and the laser signal measurement and the background measurement.
2. The nonconstant height of experimental data. It should be noted that the prediction model data were obtained assuming that the laser designator was located 10 m above the sea.
3. The errors in the experimental measurement (peak signal).
4. The simplifications made in the model.

More trials will be necessary to validate our prediction model.

8 Conclusion

Ships operating near littorals are exposed to some types of threats originally designed to engage air and land targets. Among the most important threats recently identified are the laser threats of the first and second generation, which are laser target designators and laser beamriders, portable or fully vehicle-integrated.

The high level of humidity and aerosol present in the maritime atmosphere is expected to produce more scattering in the laser signal, making it easier to detect. This significantly enhances detection performance and minimizes the number of detection heads needed to cover a warship. To determine the optimum design for the laser warning receiver and predict its performances in coastal areas, a prediction model is developed. It takes into account atmospheric content, geometrical considerations, features of the laser used for weapons guidance, and detection system characteristics. The sea-surface particle size distribution is generated according to one of the four available predefined distribution sets characteristic of coastal and maritime conditions. This one is more representative than the aerosol size distribution generated by the Shettle and Fenn model, which was used by previous off-axis scatter models, since its calculation requires 12 input parameters related to meteorological conditions and the altitude above the sea level compared to only four parameters for the Shettle and Fenn aerosol size distribution model.

Preliminary investigations show good agreement between the power collected by the laser warning receiver predicted by our model and the experimental measurements. Further analysis and trials will be required to vali-

Table 4 Mode radii for the aerosol models as a function of relative humidity.

	Rural			Urban	
Relative humidity	r_1	r_2	Maritime	r_1	r_2
0%	0.02700	0.4300	0.1600	0.02500	0.4000
50%	0.02748	0.4377	0.1711	0.02563	0.4113
70%	0.02846	0.4571	0.2041	0.02911	0.4777
80%	0.03274	0.5477	0.3180	0.03514	0.5805
90%	0.03884	0.6462	0.3803	0.04187	0.7061
95%	0.04238	0.7078	0.4606	0.04904	0.8634
98%	0.04751	0.9728	0.6024	0.05996	1.1691
99%	0.05215	1.1755	0.7505	0.06847	1.4858

date the model developed. It should be also interesting to add a background level model to perform signal-to-noise calculations.

Appendix: Background Aerosols Size Distribution Calculations

Shettle and Fenn Model

The aerosol number density distribution in the Shettle and Fenn model is represented by a sum of j log-normal distribution:[8]

$$\frac{dN(r)}{dr} = \sum_{i=1}^{j} \left[\frac{N_i}{\ln(10) r s_i \sqrt{2\pi}} \right] \exp\left[- \frac{(\log r - \log r_i)^2}{2 s_i^2} \right], \quad (18)$$

where $N(r)$ is the cumulative number density of particle of radius r; s_i is the geometric standard deviation; r_i is the mode mean radius; and N_i is the number density with r_i. For rural and urban aerosol types, two modes are generally adequate to characterize the gross features of most aerosol distributions, while for the maritime conditions only one mode is necessary. The characteristic of the aerosol model for lower atmosphere (N_i, r_i, and s_i) and the mode radii for the aerosol models as a function of relative humidity are respectively given in Tables 3 and 4.

MEDEX Model

The MEDEX background aerosol size distribution is expressed by the following equation:[9]

$$\frac{dN}{dr} = \sum_{i=1}^{i=4} \frac{A_i}{f} \exp\left\{ - C_i \left[\ln\left(\frac{r}{f r_{0i}} \right) \right]^2 \right\}, \quad (19)$$

where r_{0i} is the modal radius (r_{01}=0.03, r_{02}=0.24, r_{03}=2, and r_{04}=10 μm) and f is the growth factor related to the humidity. The coefficients A_i and C_i represent respectively the concentration (in $\mathrm{cm}^{-3} * \mu\mathrm{m}^{-1}$) and the width of the mode i. They are calculated using the following equations, where X corresponds to the fetch, X_0=3 km, and U corresponds to the wind speed:

$$A_1 = -25100 \ln\left(\frac{X}{X_0} \right) + 150{,}040,$$

$$A_2 = 10^{\{[0.0296 \ln(X/X_0) - 0.045] U - 0.385 \ln(X/X_0) + 2.1675\}},$$

$$A_3 = 10^{\{[0.046 \ln(X/X_0) - 0.0437] U - 0.465 \ln(X/X_0) - 0.523\}},$$

$$A_4 = 10^{\{[0.0095 \ln(X/X_0) + 0.0168] U + 0.1424 \ln(X/X_0) - 3.2\}},$$

$$C_1 = -0.19 \ln\left(\frac{X}{X_0} \right) + 1.679,$$

$$C_2 = -0.148 \ln\left(\frac{X}{X_0} \right) + 1.698,$$

$$C_3 = -0.295 \ln\left(\frac{X}{X_0} \right) + 2.188,$$

$$C_4 = 10. \quad (20)$$

Acknowledgments

The authors thank Denis Dion for providing the sea-surface generated particle size distribution code.

References

1. F. Reid and J. Dubois, "Surveillance and countermeasures against laser and optical threat in littoral environment," *NATO SCI-180 Symp.* SL 2006-114 (2006).
2. J. Dubois and F. Reid, "Detecting laser sources on the battlefield," *Proc. SPIE* **6796**, 67962F (2007).
3. R. C. Shirkey, R. A. Sutherland, and M. A. Seagraves, "Aerosol phase function data base PFNDAT," *EOSAEL 97, Atmospheric Sci. Lab.* **26**, TR-0221-26 (1997).
4. S. Twomey, *Atmospheric Aerosols*, Elsevier Scientific Publishing Company, New York (1977).
5. S. K. Friedlander, *Smoke, Dust and Haze*, John Wiley and Sons, New York (1977).
6. G. Roy, J. Dubois, and L. Bissonnette, "On missile guiding via atmospheric aerosol scattering," *Tech. Memorandum DRDC Valcartier*, Quebec, Canada (2003).
7. J. Dubois, M. Jones, M. Châteauneuf, J. Land, and P. Carriger, "Laser guidance for hypervelocity missiles," TTCP WPN KTA 7-13 Final Report, Unclassified, 67 pages, TR 2006-052 (Mar. 2006).
8. E. P. Shettle and R. W. Fenn, "Models for the aerosols of the lower atmosphere and the effects of humidity variations on their optical properties," ADA085951, Environmental research papers, Air Force Geophysics Lab, Hanscom AFB (1979); http://handle.dtic.mil/100.2/ADA085951.
9. J. Piazzola and G. Kaloshin, "Performance evaluation of the coastal aerosol extinction code MEDEX with data from Black Sea," *J. Aerosol Sci.* **36**, 341–359 (2005).
10. E. D. Hinkley, *Laser Monitoring of the Atmosphere*, pp. 89–90, Springer-Verlag, Berlin-Heidelberg-New York (1976).
11. *Handbook of Geophysics*, United States Air Force, pp. 16–20, New York (1960).
12. V. Ross and D. Dion, "Marine environment background synthesis using MODTRAN 4," *Proc. SPIE* **6239**, 62390H (2006).
13. V. Ross, D. Dion, and G. Potvin, "Detailed analytical approach to the Gaussian surface bidirectional reflectance distribution function specular component applied to the sea surface," *J. Opt. Soc. Am. A* **22**, 2442–2453 (2005).

Nathalie Roy received her BIng degree in physics engineering and her MSc degree in physics, realized in collaboration with the Defense Research and Development Canada Valcartier, both from Laval University, Québec, Canada in 2002 and 2004, respectively. Since then, she has created her own consulting firm specialized in gated intensified CCD camera and lidar technology. She also worked as a consultant for the Defence Research and Development Canada Valcartier before joining this research center as an engineer in 2008. Her main expertise fields are multiple field of view lidar systems, detection of small levels of signals, and the modeling of noise sources and diffusion on background aerosols.

Françoise Reid has been interested in various phenomena related to military electro-optics engineering systems at DRDC-Valcartier since 1985. She has modeled atmospheric transmission phenomena and infrared signatures of ships, and developed tools to measure the infrared signature and simulated missiles engaging ships. Several of her software realizations had an impact on the international community, one of them, ShipIR, being used as a NATO standard. She is now interested in the protection of ships against terrorism threats, when operating in littoral environments, in collaboration with our allied countries. Her interest is mainly directed at laser threats, especially laser designators and laser beamriders.